Smart Mater. Struct. **18** (2009) 104009 (10pp) doi:10.1088/0964-1726/18/10/104009

Integrity of piezoceramic patch transducers under cyclic loading at different temperatures

Monika Gall, Bärbel Thielicke and Ingo Schmidt

Fraunhofer Institute for Mechanics of Materials IWM, Freiburg im Breisgau, Germany

E-mail: monika.gall@iwm.fraunhofer.de

Received 13 January 2009, in final form 5 May 2009
Published 10 September 2009
Online at stacks.iop.org/SMS/18/104009

Abstract

In this study the loading limits, damage behavior and long-term integrity of piezoceramic patch transducers, based on monolithic PZT (lead zirconium titanate) wafers (PIC 255), were investigated. The study involved quasi-static and long-term cyclic testing under tensile and compressive mechanical loading of the patches, at different temperatures. A strain-cycle lifetime diagram was established for tensile loading at room temperature, and +60, +100 and −40 °C. In all cases of tensile loading, cracking in the PZT ceramic was found to be the relevant failure mechanism which was shown to be correlated with the observed degradation of sensor performance of the patches. No mechanical damage was found under compressive loading at strain levels of up to −0.6%. Finite element (FE) analyses were performed using 3D material modeling with electromechanical coupling, achieving very good predictability of the sensor and actuator performance. Analytical calculations and numerical simulation were used to interpret experimental findings and to allow the transfer of results to various applications. Based on micro-structural investigations of the cracked PZT wafers and FE simulation, fracture mechanics analyses of the local stress situation in the PZT ceramic were carried out.

(Some figures in this article are in colour only in the electronic version)

1. Introduction

Piezoceramic patch transducers are commercially available in a variety of designs, based on a range of piezoceramic wafers, fibers or macro-fibers which are embedded into a polymer matrix material. Such piezoceramic composites with a laminar setup are receiving increasing attention, especially for possible applications in light-weight constructions, owing to the practical advantages of distributed force transmission by surface bonding or direct embedding of the patches into the main structure (Wierach and Schönecker 2005). Further assets of the so-called PZT patches are the improved handling of the brittle ceramic due to the polymer matrix and the straightforward setup which allows for easy application-specific design optimization. The focus of the current study is the investigation of the damage behavior and long-term integrity of patches based on PZT wafers.

For any application of PZT patches in smart systems, the reliable reproducibility of sensor and/or actuator performance within an expected lifetime is indispensable. Thus, systematic investigations of their durability, loading limits and failure behavior are essential. Under working conditions, piezoceramic transducers are typically subjected to alternating electromechanical loading situations, which can eventually lead to a degradation of the mechanical and electrical properties or even to complete failure of the device. Primarily the patches have to withstand the operational demands to which their host structure is subjected, i.e. the basic mechanical loading and environmental conditions.

Previously, many studies on the integrity of smart structures concentrated solely on the influence of embedded actuators/sensors on the strength and fatigue behavior of the host structure, often using dummy actuators in the testing. On the other hand, most studies of piezoceramic fatigue were carried out on the pure piezoceramic bulk material, which neglects influences from the structure–actuator/sensor interaction. One of the first studies to focus on the integrity of active PZT wafers actually embedded into fiber reinforced

composite structures was presented by Bronowicki *et al* (1996), studying navy type I and II PZT wafers under axial tensile and compressive cyclic loading followed by thermal cycling. A study on ACX-PZT patches embedded into graphite epoxy laminates was carried out by Mall and Hsu (2000) and Mall (2002), studying the integrity of the primary structure under high tensile strain and the patch integrity at lower strain levels. Additionally combined electromechanical loading was investigated. This study was extended by Yocum *et al* (2003) by adding fully reversed tension–compression fatigue testing combined with fully reversed electric cycling. Finally Edery-Azulay and Abramovich (2007) extended this study by testing surface mounted samples of bare PIC 255 PZT wafers in addition to the embedded setup, as well as various combinations of symmetric and asymmetric setups in axial tensile and compressive electromechanical loading. Recently, Nuffer *et al* (2008) presented works on the integrity of wafer-based PZT patches for high temperature applications which were submitted to various electrical and mechanical cyclic loading conditions at temperatures up to +150 °C.

With the exception of the latter, these studies focused mainly on the changes in the sensor or actuator performance during the tests. Investigations of typical damage patterns were not reported and conclusions as to the underlying failure mechanisms were largely drawn from interpretation of the performance degradation in context to the applied loading conditions. This was probably at least partially due to the embedment of the samples in the test structures, constricting the possibilities of directly monitoring the patch condition.

In the current study, however, a strong focus was laid on the investigation of typical damage patterns. This is to provide a straightforward approach for directly linking an observed performance reduction to a specific failure mechanism, allowing in the end to formulate a mechanism-based model for lifetime prediction. For this reason only surface mounted test specimen were used in this study. Also, rather than investigating a large variation of possible combined loading situations, the testing conditions were specifically chosen to be rather basic, to keep cause-and-effect as traceable as possible.

The current study is a continuation of investigations first presented by Poizat *et al* (1999) and Thielicke *et al* (2003), where the use of the 4-point bending test setup was proposed as a simple, but highly effective method to study the sensor performance of piezoelectric composites on various substrates. These studies were extended by Gall and Thielicke (2007), who investigated the long-term integrity of wafer-based PZT patches and presented a lifetime diagram for tensile loading at room temperature (RT).

As detailed in the following, the testing program was extended to investigate the influence of temperature on the damage behavior and lifetime of the patches. The chosen temperatures (+60, +100 and −40 °C) cover a wide range of temperatures which are of practical relevance in a variety of possible fields of application (e.g. automotive and biomedical engineering). As a result, an extended temperature-dependent lifetime diagram for tensile loading is presented.

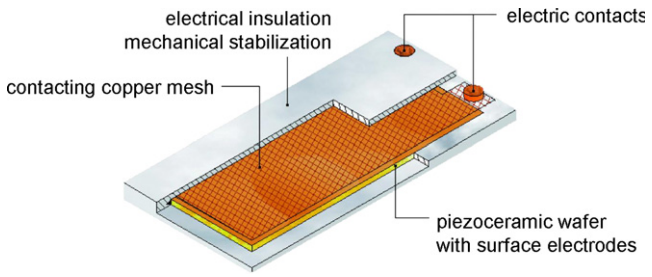

Figure 1. Setup of pre-encapsulated PZT patches (Wierach *et al* 2002).

Furthermore the accompanying micro-structural, analytical and numerical investigations were continued and new results, including fracture mechanics analysis, are presented and discussed.

The overall goal of this study is to provide potential users of the PZT patches with the needed information on expected performance and lifetime under given application-specific loading conditions. In the long run, the objective is the development a mechanism-based model for lifetime predictions of PZT sensors/actuators under various loading conditions, combining the results from experimental, analytical and numerical studies.

2. Design of PZT patches

The PZT patches investigated in this study (see figure 1) are based on monolithic piezoceramic wafers. The PZT wafer material is PIC 255 (by PI Ceramic), the standard wafer size of the investigated samples was 50 × 25 × 0.2 mm^3. The top and bottom sides of the ceramic are uniformly covered with sputtered surface electrodes of a few nanometers thickness, to operate the patch in the lateral extension mode (d_{31}-mode). As described in more detail by Wierach *et al* (2002) the surface electrodes are covered by a contacting copper mesh which is connected to the electric contacting points. The ductile copper mesh can electrically bridge defects of the surface electrodes, caused, e.g., by cracking of the PZT ceramic. Thus the patches can still be operated even if some cracking has occurred. The PZT wafers with the complete contacting and a thin layer of insulating fiber material are pre-encapsulated in an epoxy resin matrix. This provides electrical insulation and also mechanical stabilization and protection of the brittle piezoceramic. The resulting total thickness of the investigated patches was 0.43 mm.

3. Experimental setup

3.1. Sample preparation

For lifetime investigations the PZT patches were applied to suitable substrates, to simulate the loading situation in real applications. For testing under mechanical loading at various strain amplitudes a carbon fiber reinforced polymer (CFRP) material was found to be convenient. In contrast to steel substrates, the CFRP material shows elastic behavior up to 0.6% strain, allowing for cyclic testing at such strain levels.

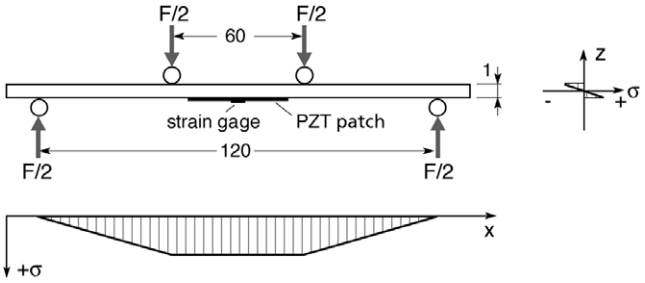

Figure 2. Dimensions (in mm) and loading principle of 4-point bending test (setup for tensile loading).

3.2. 4-point bending setup for tensile and compressive loading

4-point bending of the substrate leads to tensile or compressive loading of the PZT patch depending on the side of the substrate to which the patch is applied (Poizat *et al* 1999). Figures 2 and 3 show the principle and a photograph, respectively, of the setup oriented for tensile loading. The PZT patches were surface bonded onto the center of a CFRP substrate of 140 × 30 × 1 mm^3 dimension (figure 3(b)). The bending fixture was adapted to match the patch length, such that the patches were positioned in the zone of constant bending moment between the inner loading rollers. As the patches are relatively thin compared to the substrate, nearly homogeneous strain and stress can be assumed in the PZT wafer. Turning the specimen around, to make the PZT patch face up, will apply compressive loading to the patch, thus offering a convenient way to perform compressive testing without the problem of buckling.

A BOSE EnduraTEC ELF 3200 testing machine was used to apply displacement controlled mechanical load to the specimens. As shown in figure 3, strain gages were glued on the PZT patches, so the loading could be controlled to reach the desired strain levels in the patches.

In addition to monitoring the machine displacement, the load and the strain at the gage, the electric sensing signal of the patches, which is the electric charge on the PZT wafer, produced under mechanical strain through the piezoelectric d_{31}-effect, was measured (KISTLER 5001 charge amplifier).

To study the influence of temperature on the patch behavior and lifetime, the 4-point bending test was installed in a conditioning chamber, which fits into the setup of the testing machine. For testing at elevated temperatures the chamber is equipped with an integrated heating system. For cooling an external liquid nitrogen reservoir was connected to the chamber.

4. Testing procedures and control of sample condition

4.1. Repolarization procedure

Prior to any testing, the specimens were subjected to a voltage of +400 V, corresponding to an electric field of +2000 V mm^{-1}, for 1 min. This procedure, referred to as 'repolarization', was used to secure an identical initial polarization state of the PZT wafers in all samples.

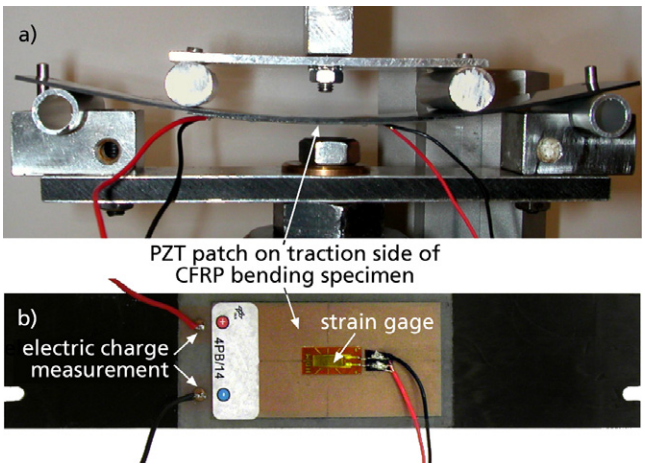

Figure 3. Test setup with PZT specimen under tensile loading (a) and view of patch on CFRP substrate (b).

4.2. Monitoring of sample condition

The health of the patches was monitored by a combination of visual inspection (stereo microscopy) and the evaluation of the measured electric charge and strain data. Since the measured electric charge is a direct result of mechanical strain in the PZT wafer through the direct piezoelectric effect, the slope of the charge-versus-strain curves directly characterizes the sensor performance of each individual patch. A reduction of the slope of the measured charge–strain curves constitutes a degradation of the sensor performance. Thus the slope value can be used as a direct measure of the sample condition.

In contrast to visual controlling, for which the samples have to be taken out of the testing setup, charge–strain curves of a sample can be evaluated *in situ*, without interrupting the test.

4.3. Quasi-static and cyclic mechanical loading

In the quasi-static tests the bending specimens were subjected to a ramp-like loading–unloading procedure with stepwise increasing maximum strain levels, starting with the first ramp to 0.08% strain and going up to nearly 0.6% strain in the final ramp (in compressive testing: −0.08% up to −0.6%, respectively). The quasi-static loading procedure was employed to investigate the loading limits and typical damage patterns under tensile and compressive loading.

To study the long-term behavior of the patches under mechanical loading, cyclic testing in a sinusoidal loading program was used. The amplitude of the machine displacement was regulated such that the maximum applied strain level was set at a value between 35% and 70% of the loading limit determined in the quasi-static test. The minimum displacement was set at a very low, but non-zero value, to avoid lift-off of the loading rollers. Testing frequencies below 10 Hz were chosen to reduce the rate dependency of the results. Typical test periods were three days up to one week. Since continuous recording would have produced enormous amounts of data, control measurements were performed at preselected intervals. These measurements included quasi-static ramp loading as

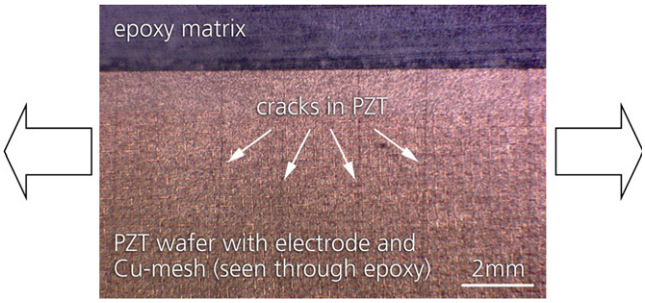

Figure 4. PZT patch with cracks running perpendicular to loading direction after tensile testing: uniformly electroded surface of PZT wafer with cracks can be seen through the covering copper mesh and epoxy layer (detail of top view, 6× enlarged).

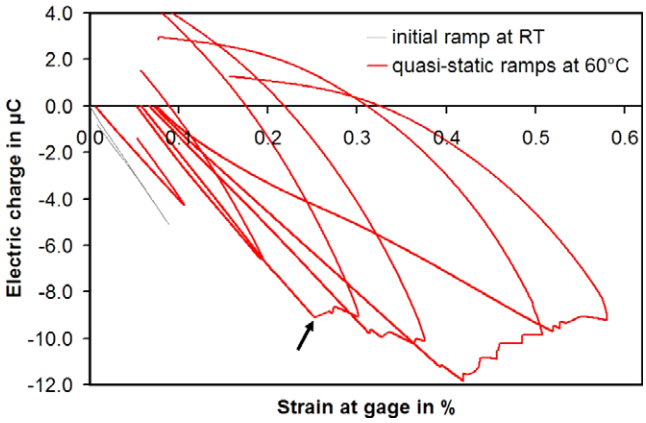

Figure 5. Charge–strain curves in quasi-static ramp testing with stepwise increased maximum strain for sample tested at +60 °C: kinks indicate cracking of PZT wafer.

well as recording of several sinusoidal loading cycles, the data was evaluated in charge–strain curves. At RT the control also included visual inspection.

4.4. Tensile testing at different temperatures

In addition to the tests at RT, tensile tests were also performed at +60, +100 and −40 °C. Before the heating/cooling was started, the initial condition of the samples at RT, after the repolarization procedure, was recorded by performing a quasi-static ramp test up to 0.08% strain. Also a control ramp was performed at RT directly after the tests were finished, followed by renewed repolarization and another control ramp at RT. These RT control ramps were necessary for a direct comparison of the specimen condition, since the charge–strain curves were slightly temperature-dependent.

5. Experimental data and results

5.1. Loading limits and typical damage behavior under tensile loading

In quasi-static tensile testing at RT, it was found that at an average strain level of 0.35% cracks occurred in the PZT wafers (Gall and Thielicke 2007). As the quasi-static testing was continued up to higher strain levels, a growing number of cracks was noted in the visual inspections after each ramp. Also, the occurrence of cracks was audible during the testing.

The cracks were found to run perpendicular to the tensile loading direction (see figure 4). Microscopic surveys of the samples revealed no evidence of further damage, such as delamination between the patch and the substrate or within the patch itself, which could be anticipated at elevated strain levels.

Also all electric contact points were still intact. Due to the copper mesh bridging the damaged surface electrodes of the cracked PZT wafers, the cracking of the wafers did not lead to a complete breakdown of the patches. In the evaluated charge–strain-curves of the samples after the tests, a severe drop of the sensor performance was registered.

Analogous results were observed in quasi-static tensile testing at all temperatures investigated in this study: cracking of the PZT wafer was always found to be the relevant damage mechanism, and no other damage could be found under microscopic inspection.

While in the RT tests the specimens were visually inspected for damage after each loading–unloading ramp, this was not possible at elevated or reduced temperatures. It would have meant a repeated cooling/heating process of the samples in the conditioning chamber, which could cause additional changes of the sample condition and therefore was avoided. Thus only after completing the tests in the conditioning chamber, the samples could be visually inspected. Therefore, the charge and strain data was continuously recorded in the quasi-static tests at temperatures other than RT. (At RT only the initial state and the performance after completing the test were recorded as additional information to the visual inspection.)

Figure 5 shows the charge–strain curves measured on a specimen tested at +60 °C in quasi-static ramps up to stepwise increased maximum strain levels. In the tests at +60 °C the occurrence of cracking was again audible and could be exactly related to kinking of the charge–strain curves (the first cracking kink in the diagram is marked by the arrow). The diagram clearly shows that the occurrence of cracks (as indicated by kinking of the curves) is followed by a distinct reduction of the slope of the next loading–unloading curve, marking a degradation of the sensor performance of the sample. After the first cracks, the curves still show nearly linear behavior in the loading part of the curve, up to crack occurrence. The unloading paths of the curves show more or less nonlinear behavior for all tests. High strain levels clearly lead to increased cracking. The last curve exhibits markedly nonlinear characteristics also in the loading part.

At higher temperatures, as well as at −40 °C, cracking could not be heard due to the higher noise level of the fan in the conditioning chamber. Still, the charge–strain curves exhibited the same characteristic kinking, followed by a reduced slope in the next loading–unloading ramp. After the testing program cracks could be seen in the PZT wafer of the samples.

Generally, testing at higher temperatures resulted in reduced slopes of the curves as compared to RT curves, i.e. at the same strain levels measured at the strain gages on the patch surfaces, the embedded PZT wafers produced a lower

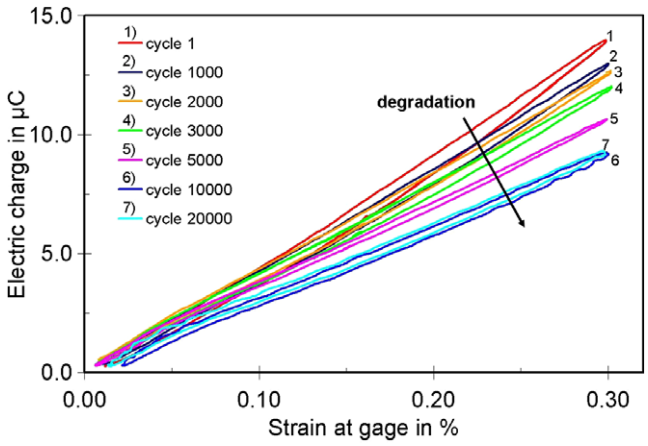

Figure 6. Charge–strain curves of a specimen under cyclic fatigue testing at a maximum strain level of 0.3% at RT.

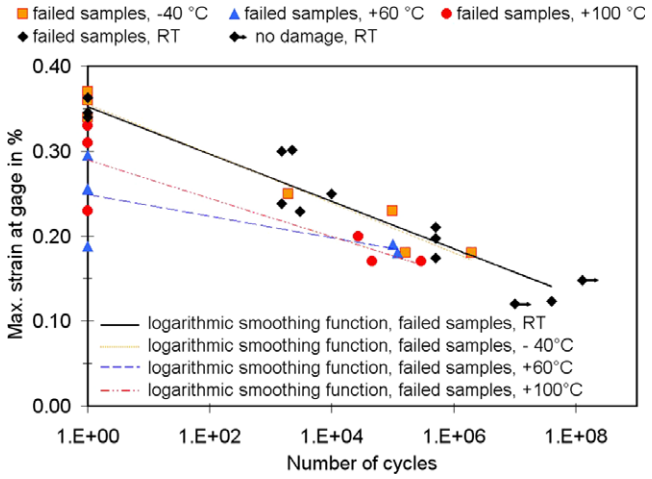

Figure 7. Fatigue life diagram for mechanical tensile loading of PZT patches at different temperatures.

electrical charge output. At 120 °C the sensor performance of the patch was found to be extremely diminished, so testing at this temperature level was discontinued. At −40 °C the curves exhibited very similar characteristics and slopes as at RT.

For the evaluation of the test data in a lifetime diagram (see section 5.3), a degradation of the sensor performance below 90% of the initial performance was specified as failure criterion. Accordingly, samples from quasi-static testing were regarded as failed if the slope of the charge–strain curve in the next loading–unloading ramp was less then 90% of the initial slope of the first curve measured at the testing temperature.

The loading limit of a sample was determined as the strain at the first kink of the curve before the failure criterion was reached. In most samples, this was the first cracking kink that occurred, like the point marked by the black arrow in figure 5. (Since in RT testing no continuous charge–strain curves were recorded, the occurrence of the first crack, as acoustically observed, was used for the determination of the loading limit.) As mentioned before, the average loading limit at RT was determined at 0.35% tensile strain (4 samples, black diamonds in figure 7). At elevated temperatures the loading limits tended to be below the value at RT: at +60 °C the average loading limit was determined as 0.25% strain (4 samples, blue triangles), and at +100 °C as 0.29% (3 samples, red dots). The average loading limit at −40 °C was found to be 0.36% tensile strain (3 samples, orange squares), which was slightly above the one at RT. It is noteworthy that a much higher scatter of the quasi-static failure data points was observed at elevated temperatures as compared to RT and −40 °C. Also, it is somewhat unexpected that the average loading limit at +60 °C was smaller than at +100 °C, but regarding the high scatter in both data sets, the difference is not significant.

5.2. *Cyclic fatigue life testing*

At RT all samples that were tested in tensile cyclic loading at strain levels above 0.12% showed a degradation of the sensor performance characterized by a slope reduction of the charge–strain curves. Also intermediate visual controls revealed an increasing number of cracks in the PZT wafers as the cyclic testing of the samples proceeded. Figure 6 represents the typical degradation pattern of the charge–strain curves of a specimen under tensile cyclic loading. This specimen was tested at a maximum strain level of 0.3% at RT.

If the slope of the intermediately recorded control curves was more than 10% lower than in the initial reference curve (first cycle) of the sample, the specimen was considered failed (see section 5.3 for more details on failure criterion). As expected, in cyclic testing at lower strain levels, the degradation of the sensor performance and cracking occurred at lower rates, resulting in a higher number of cycles before failure. This general observation was true for all testing temperatures.

Several samples tested at +100 °C developed a smaller number of cracks than the other samples, even though they exhibited a similar reduction of the slope of the control charge–strain curves. The samples with a very small number of cracks also showed a tendency towards recovery of the sensor performance, some almost reaching the initial condition after a renewed repolarization process. This was not the case in samples with a higher number of cracks.

5.3. *Temperature-dependent fatigue life diagram*

Based on the evaluation of quasi-static and cyclic tensile testing at RT a lifetime diagram characterizing strain-cycle correlations was established by Gall and Thielicke (2007). This diagram was now complemented with the temperature-dependent test data. The resulting temperature-dependent lifetime diagram is shown in figure 7. The maximum of the applied strain is plotted versus the number of cycles that was reached before failure occurred.

A specimen was regarded as failed if the sensor performance dropped below 90% of the initial state value. The same failure criterion was already used for the fatigue life diagram under tensile loading at RT. In comparison to failure criteria used by other research teams, failure at a reduction to 90% of the initial sensor performance is a rather narrow limitation. Mall (2002), for example, considers a sample

as failed, if the sensor performance drops below 50%, and again to 70% of the initial performance after an intermediate repolarization. In this work the 90% critical value was chosen to allow only relatively small deviations from the designated sensor/actuator performance of the patches. This was decided in view of the intended application of the patches in so-called smart structures, where stable performance is a necessity for the application of straightforward, non-adaptive control algorithms. It has to be borne in mind that in this context, the term failure refers only to the reduction of sensor performance as specified in the failure criterion, not to a complete breakdown of the patch properties. As mentioned before, the patches will still function after the occurrence of cracks, due to the electrical contacting copper mesh.

The data points on the vertical axis represent the loading limits in the quasi-static tests. The straight lines in figure 7 represent fits to the data points for each test temperature, including the quasi-static results. These fatigue life curves provide a basis for long-term reliability predictions of the patches.

As already observed in the quasi-static tests, in long-term cyclic testing, too, a reduction of the sustainable strain was found at elevated temperatures. As a result, the lifetime curves at +60 °C (blue dashed line) and +100 °C (red dashed–dotted line) both lie below the RT curve (black solid line). As in the quasi-static tests, the fatigue lifetime at −40 °C does not differ markedly from the results at RT, yielding a lifetime curve (orange dotted line) which is almost identical to the RT curve.

The black arrow mark at a maximum strain level of 0.12% represents several samples which were tested for 10^7 cycles at RT without failure. This was tested in fulfilment of the specifications put up when the patches were newly designed in the German project 'Adaptronics' (Wierach *et al* 2002, Thielicke *et al* 2003).

5.4. Reliability under compressive mechanical loading

Quasi-static and cyclic testing under compressive mechanical loading at RT was discussed in detail by Gall and Thielicke (2007). Since no additional data is presented here, the results will only briefly be reviewed to complete the information on the behavior of the PZT patches under mechanical loading.

Under compressive loading the measured electric charge of the PZT patches was of opposite sign in comparison to tensile testing. Besides, the charge–strain curves showed reduced slopes and reached lower absolute charge values at the same absolute strain levels. Even at low absolute strain levels (<0.1%) the charge–strain curves exhibited nonlinear behavior. With increasing strain levels, the nonlinearity became more pronounced, and the peak amplitudes degraded. In spite of this obvious degradation of the sensor performance, no signs of mechanical damage could be found after quasi-static testing at strain levels of up to −0.6%. In cyclic testing the samples reached up to 10^5 cycles at −0.6% strain and 10^7 cycles at −0.35% strain without any sign of mechanical damage. The tests were then discontinued. After the compressive tests the samples were repolarized (1 min at +400 V) and again showed the initial sensor performance in tensile control ramps as before the tests.

Figure 8. Sample with asymmetric setup: only bottom side of PZT wafer is covered by copper mesh and epoxy resin, resulting in bending after thermosetting process of resin.

As an additional reference value, the electric capacitance of the samples was controlled throughout the compressive testing program. During the test the capacitance exhibited a similar degradation as the sensor performance and also showed complete recovery after repolarization. Interestingly the capacitance partly recovered already after a first tensile test ramp was performed, even before repolarization.

6. Analytical and numerical investigations and results

6.1. Analytical investigation of residual stresses

During manufacturing of the PZT patches, the unequal shrinkage of the thermosetting epoxy resin and the PZT ceramic results in a compressive pre-stressing of the PZT wafer, which has a favorable effect on the tensile strength of the patches. To appraise the magnitude of the compressive residual stresses in the PZT, several patch samples were prepared with epoxy resin only on one side. This asymmetric setup was then thermally processed exactly like the regular patches, that is, letting the resin set at 110 °C and then cooling the samples down to RT.

Due to the asymmetric setup, the unequal shrinkage of the materials resulted in a curvature of the samples as shown in figure 8. This was measured and by means of bending theory the stress in the regular patches was analytically calculated to be of the order of 20 MPa.

Heating of the PZT patches would then result in a proportional reduction of the compressive residual stresses. At +100 °C this should result in an effective reduction to 1/10th of the residual stress magnitude at RT.

6.2. FE simulation of 4-point bending test

In conjunction with the experimental test program, finite element analyses were carried out to help the interpretation of experimental results and to provide a tool for predicting the actuation and sensor performance of the PZT patches. In the analyses ABAQUS 20-node brick elements were used, featuring linear piezoelectric coupling in the PZT wafer (C3D20E) and simple elasticity in the other materials (C3D20: epoxy, CFRP substrate). Electrical boundary conditions (BC) linked the electric potential at all nodes of each of the PZT wafer surfaces, modeling the surface electrodes which are electrically conducting. The top electrode was grounded by setting the electric potential equal to 0 V. At the other electrode

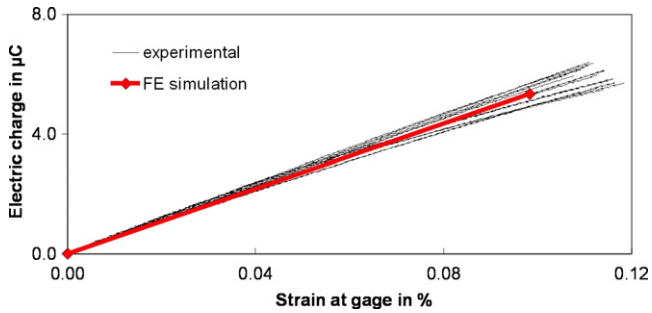

Figure 9. Charge–strain curves of undamaged specimen under tensile loading in 4-point bending test: comparison of experimental results (black curves) and FE simulation (red diamonds and line). It is notable that even in the so-called small strain regime (here: up to 0.1% strain) the piezoelectric sensor performance of the samples showed slightly nonlinear characteristics. The resulting deviation between linear FE results and experimental data is not significant in view of the scatter of the experimental data, however.

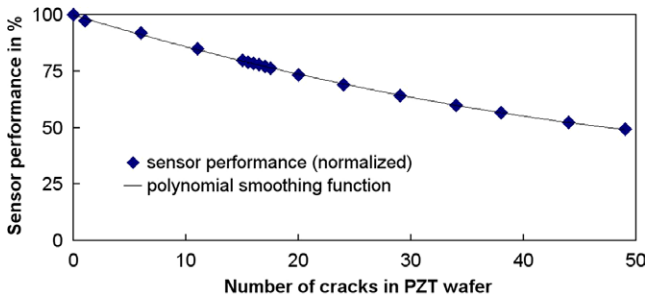

Figure 10. Normalized sensor performance of 2D model of PZT patch with varied number of cracks in PZT wafer: increasing degradation of sensor performance due to reduced strain in PZT fragments with rising number of cracks.

the voltage output could be derived in the bending test (sensor application) or a voltage could be applied to simulate actuator applications. To compare the results of the FE simulation to the experimentally measured electric charge in the bending test, the electric charge ΔQ was calculated from the resultant electric potential at the free electrode, using the capacitor analogy (A = surface area of one electrode, d = PZT thickness, $\varepsilon_{(S)33}$ = dielectric permittivity at constant strain)

$$\Delta Q = \varepsilon_{(S)33} A \frac{(\varphi_{\text{bot}} - \varphi_{\text{top}})}{d}. \tag{1}$$

Good agreement between experimental data and FE results were achieved for tensile 4-point bending tests at strain levels up to 0.1% (as shown in figure 9) as well as for a bending actuator setup (as described in more detail by Gall and Thielicke 2007).

By reversing the mechanical loading direction, the compressive bending test was simulated. Here it was interesting to note that this loading condition leads to a negative electric field in the PZT patch. This supported some ideas about the reversible degradation of the sensor performance occurring in the compressive testing procedure (see section 7).

6.3. Numerical investigation of sensor degradation due to cracks in PZT patches

Additional numerical studies were carried out to investigate the correlation between the sensor degradation of the patches and the number of cracks in the PZT wafer. A 2D plane stress beam model was used to simulate a range of 1–50 cracks in the PZT wafer. Assuming the ideal case of uniformly distributed cracks over the length of the wafer, a certain number of cracks correspond to a characteristic length of the PZT wafer fragments. In the 2D model, a representative section of the PZT patch was considered, from the middle of one fragment to the middle of the next fragment, which encompassed one crack in the PZT. The PZT fragment and two layers of epoxy above and below the PZT, were modeled with bilinear plane stress elements (piezoelectric CPS4E and elastic CPS4), for the CFRP substrate a series of 1D truss elements (T2D2) was used. Due to the system symmetry, only one half of the representative section was modeled. In the crack-plane symmetry boundary conditions were applied for the epoxy and CFRP layers in length direction. By leaving the PZT layer unrestrained, modeling of the crack was achieved. The approximatively uniaxial tensile strain loading of the PZT patch in the 4-point bending setup was modeled by applying a uniform displacement in length direction to the free end of the model, resulting in a homogeneous strain of 0.1% in the reference model without crack (additional symmetry BC in length direction on PZT layer).

As the evaluation showed, the model without crack was homogeneously strained, whereas, in the crack model, the epoxy layers in the region close to the crack were strongly strained, while the PZT layer was experiencing very low strain in the proximity of the crack. This resulted in a lower overall strain in the PZT, returning a lower piezoelectric sensor output than the model without crack.

Different numbers of cracks were modeled by varying the length of the model. The electric charge collected from one fragment of PZT can be derived from equation (1). Since the total resulting electric charge for the complete patch is the sum over all fragments (by fragment area), the sensor performance could be directly compared by comparing the electric potential output for all models.

Although, due to the model simplifications, the absolute value of the calculated electric charge did not directly fit to the experimental results, the relative degradation of the sensor performance at a certain number of cracks did correspond well. The evaluation of the 2D model variations (diagram figure 10) shows a degradation to about 75% of the initial sensor performance in a patch with 15–20 cracks. This was in found to be in good agreement with the experimental results from tensile test samples in quasi-static ramps at RT, for which the number of cracks was counted under the microscope. By using the symmetry BC alteration in the 3D bending model (no symmetry BC in the PZT in length direction), the

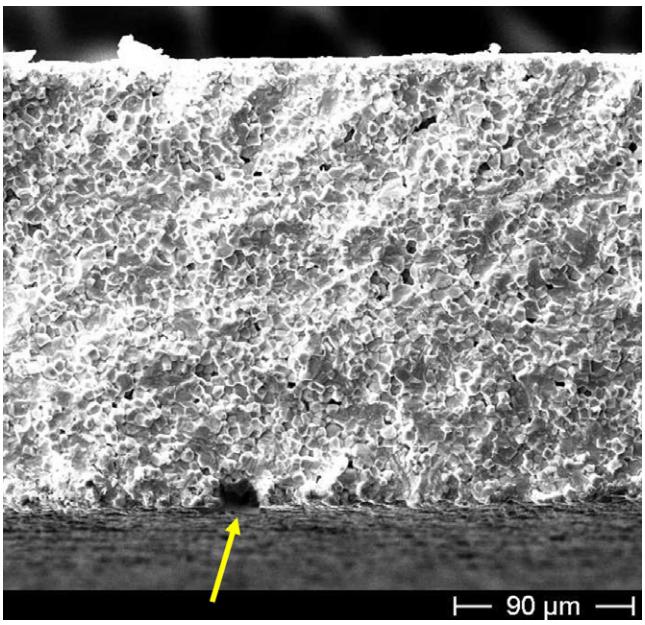

Figure 11. SEM image of fracture surface of PZT wafer with defect (arrow).

sensor degradation for one crack could easily be evaluated and confirmed the 2D results.

6.4. Fracture mechanics approach

The key factors in fracture mechanics analyses of crack propagation are the shape, geometry and location of defects, as well as the geometry and loading situation of the sample itself. If a defect lies in a region with high tensile stresses and exceeds a certain critical size, it will be the starting point of a crack. Therefore micro-structural investigations of the samples were necessary to be able to accurately describe the existing defects.

6.4.1. Micro-structural investigation of cracked PZT wafers. The aim of these investigations was to look for the crack origin in the fracture surfaces of damaged specimen from the tensile mechanical testing program at RT. Thus the critical defect geometry and size could be determined. To study the fracture surfaces, they had to be separated by removing the epoxy resin and the CFRP substrate from the samples. This was achieved by pyrolysis as suggested by P Ditas (PI Ceramics, Germany). The complete sample was heated to 500 °C for several hours, leaving only the PZT wafer with the copper mesh still loosely attached to the electrodes. From the copper mesh the single PZT fractions could be detached and prepared for scanning electron microscopy (SEM). The SEM image in figure 11 shows a defect on one surface of the PZT wafer, which might have been the origin of a growing crack. The defect is of nearly semi-circular form, with a diameter of about 18.5 μm. The image also shows several other pore-like defects, but all of those have much smaller radii (2–6 μm) and are situated in the body of the ceramic wafer, which is a less critical location than close to the surface.

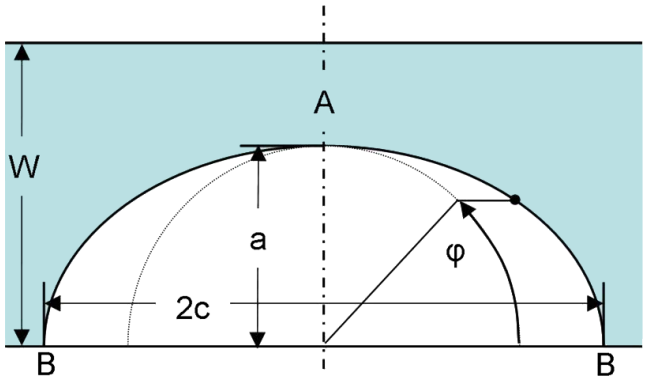

Figure 12. Geometrical data for semi-elliptical surface crack in a plate (Fett and Munz 1997).

6.4.2. Application of fracture mechanics handbook solutions for cracking under tensile load. Since the basic setup of the PZT wafer in the patches and the 4-point bending test provide a rather simple geometry and loading situation, it was possible to apply handbook formulae for the evaluation of the stress intensity factor, which characterizes the local stress concentration at a defect. A handbook solution for semi-elliptical surface cracks in flat plates under tension and bending as described by Fett and Munz (1997, pp 275–277) was applied to the defect shown in figure 11. The geometry considered in this solution is given in figure 12.

The stress intensity factor K_I was calculated from the formula for tensile loading of the plate

$$K_I(\varphi) = \sigma\sqrt{\pi a}F(\varphi), \tag{2}$$

where F is a geometric function of φ, a/c and W/a. Values for F can be derived e.g. from table 71 in Fett and Munz (1997, p 277). In the defect found in the PZT wafer the respective dimensions were: $2c = 18.5$ μm, $a = c$ (semi-circle) and $W = 200$ μm. For the calculation of the most critical value, K_I was evaluated at point B with $\varphi = 0$ (as shown in figure 12).

The tensile stress was taken from FE simulation of the 4-point bending test. For a loading situation with 0.347% tensile strain (average failure strain in quasi-static tensile tests at RT) in the epoxy embedding at the location of the strain gage on the real sample, the resulting maximum tensile stress on the lower surface of the PZT was 237.4 MPa. From this 20 MPa were subtracted to account for the compressive residual stresses resulting from the manufacturing process, yielding a final value of 217.4 MPa tensile stress. Due to the small thickness of the PZT wafer compared to the total thickness of the bending specimen, the loading situation was in good approximation assumed as pure tensile loading.

The resulting calculated stress intensity factor was

$$K_I = 0.866\ \text{MPa m}^{1/2}.$$

This value is in good agreement with critical stress intensity factor values from experimental fracture mechanics testing of PZT PIC 151 ceramics with poling in crack growth direction, as presented by Santos e Lucato *et al* (2000). No fracture data for PIC 255 was available, but according to Felten

(2008), no large difference would be expected between the two materials in the considered case, without any additional electrical loading.

7. Discussion

On the basis of the presented experimental results, cracking in the PZT wafer was identified as the relevant damage mechanism of the patches under tensile loading at all investigated temperatures. FE studies of patch models with cracks in the PZT wafer confirmed the correlation of sensor degradation with crack density. Thus it is concluded, that the reduction of the sensor performance of the patches is basically the result of the cracking of the PZT wafer, which reduces the mechanical stiffness of the PZT patch and thereby decreases the actual strain in the PZT wafer. A lower strain in the PZT then naturally produces a reduced charge output. This attribution of sensor failure mainly to the PZT cracking is opposed to the idea of possible mechanically induced depolarization effects, which was suggested by Mall and Hsu (2000). It is also supported by the fact that the sensor performance of the samples could not be recovered by electric repolarization.

Due to the importance of cracking, micro-structural investigations and fracture mechanics analyses were performed. The analysis of a preexisting defect in the PZT wafer under quasi-static testing conditions yielded a stress intensity factor which is in good agreement with results from the literature. This shows that the applied models, even though they are rather straightforward, are already accurate enough for a prediction of the loading limit for the patches under quasi-static tensile loading at RT.

Studying the influence of temperature on the patch performance and fatigue behavior, a general reduction of the sensor performance at elevated temperatures was observed. This can be at least partially explained by the temperature induced softening of the epoxy matrix and adhesive, leading to a decrease of the strain transmitted to the PZT wafer. Moreover, in the quasi-static and cyclic testing at $+60$ and $+100\,^{\circ}\mathrm{C}$, a reduction of the maximum sustainable tensile strain level was found, resulting in lifetime curves which lie below the RT curve. This reduction of the loading limit and fatigue lifetime can be attributed to the temperature related relaxation of the production induced compressive residual stresses in the PZT wafer (which have a favorable effect on the tensile strength of the device at RT), though closer studies will be needed to quantitatively relate the different mechanisms involved.

Finally, at elevated temperatures, several samples showed a lower number of cracks after tensile testing than RT samples, while both types showed the same reduction of sensor performance. Also, in those samples the sensor degradation proved to be at least partly reversible by electrical repolarization. This gives rise to the assumption that at elevated temperatures in addition to the cracking damage mechanism, a second, temperature-dependent mechanism causes reversible depolarization, even though the tested temperature levels were well below the temperature limit of $+150\,^{\circ}\mathrm{C}$ (less than half the Curie temperature of PIC 255 at $+350\,^{\circ}\mathrm{C}$) suggested by the manufacturer of the patches.

Under compressive loading distinctly higher strain levels could be sustained by the patches than under tensile loading. This tendency generally could be expected since ceramics are typically more sensitive to tension than to compression. Even at a maximum strain amplitude of -0.6% no mechanical damage was detected in quasi-static and cyclic tests. The degradation of the slopes and amplitudes of the charge–strain curves, which was observed at increasing compression levels, was found to be reversible by repolarizing the piezoceramic wafer. These results suggest that the performance degradation under compressive loading is related to reversible depolarization in the PZT material, as opposed to permanent damage mechanisms like the cracking of the PZT wafer under tensile loading. This idea is supported by the fact that in the FE analysis a negative electric field is found in the PZT under compressive loading, which would in turn depolarize the ceramic.

8. Conclusion

The 4-point bending test setup and the quasi-static and cyclic testing procedures have proven to be expedient tools for the investigation of the integrity of laminate piezoelectric transducers under various mechanical loading and ambient conditions. The strain-cycle lifetime diagram of the investigated wafer-based PZT patches for tensile loading at RT was successfully extended to cover a temperature range from -40 to $+100\,^{\circ}\mathrm{C}$. At all investigated temperatures, cracking of the PZT wafer was identified as the relevant damage mechanism, causing significant degradation of the sensor performance. Failure was defined as degradation of the sensor performance below 90% of the initial value.

At RT the average loading limit which caused instantaneous failure was determined at 0.35% tensile strain. At elevated temperatures the loading limits were found to be reduced (at $+100\,^{\circ}\mathrm{C}$ about 20% lower than RT). Also, in the cyclic testing at elevated temperatures, a reduction of the sustainable strain was found. At $-40\,^{\circ}\mathrm{C}$ all testing results were found to be very close to RT data.

Due to the small number of specimens tested at each temperature and the high scatter of the results, the derived temperature-dependent fatigue life curves may not be directly used for lifetime predictions at varied temperatures. But they do show clear trends which should be considered in the dimensioning and design of planned applications.

Under compressive loading up to -0.6% strain could be sustained by the patches without any mechanical damage. Due to the strongly nonlinear characteristic of the charge–strain curves at compressive strain levels above 0.25% absolute value, this range is not recommended for sensor application of the patches. Progressive sensor degradation was observed for increasing compressive strain, but was found to be reversible after repolarization.

Based on micro-structural investigations of the cracked PZT wafers and FE simulation, fracture mechanics analyses of the local stress situation in the PZT ceramic were carried out

and results were found to be in good agreement with literature data. Numerical investigations showed good agreement between the experimental data and simulation results and proved to be a practical tool to help interpret experimental findings. Even though the currently available commercial tools provide only linear piezoelectric material models, a good predictability of attainable results for applications of piezoelectric actuators/sensors in smart structures can be achieved.

9. Outlook

The long-term objective of this study is the development of a mechanism-based model for lifetime predictions of the PZT patch transducers under various loading conditions, combining the results from experimental and analytical or numerical studies. As presented here, the experimental testing program has already yielded interesting results, which show that fracture mechanics with regard to studies of piezoceramics is of high interest. One of the main focuses of the future works will be to analyze the presented tensile fatigue testing results in terms of fracture mechanics models for fatigue crack growth. Also, the temperature related reduction of sensor performance and sustainable strain level as well as the observed partial recovery of sensor performance through repolarization in some of the high temperature samples will be more closely investigated.

As expressed in several publications on fracture research in ferroelectrics, due to the coupling effects of mechanical and electrical fields, it is necessary to consider not only the stress intensity factor (K_{I}) but also an electrical field intensity factor (K_{IV}), especially if mixed mechanical and electrical loading situations are present. This is subject of ongoing studies in this project.

Acknowledgments

Financial support by the German Research Society DFG in the program 'Adaptronics in Machine Tools' is gratefully acknowledged. The authors would like to thank P Ditas from PI Ceramic in Lederhose, Germany for suggesting and carrying out the pyrolysis procedure necessary for micro-structural crack-face investigations. We also very much appreciate the good cooperation with P Wierach and his group from DLR in Braunschweig, Germany, who provided the samples for testing, and with S Linke from Invent GmbH, Braunschweig, Germany, who provided the asymmetric setup samples for residual stress investigation. Also, the valuable dedication of several colleagues at the IWM in Freiburg to different parts of the experimental testing program is gratefully acknowledged. Last but not least, the authors want to thank Marc Kamlah for the fruitful discussions.

References

Bronowicki A J, McIntyre L J, Betros R S and Dvorsky G R 1996 Mechanical validation of smart structures *Smart Mater. Struct.* **5** 129–39

Edery-Azulay L and Abramovich H 2007 The integrity of piezo-composite beams under high cyclic electro-mechanical loads—experimental results *Smart Mater. Struct.* **16** 1226–38

Felten F 2008 private communication

Fett T and Munz D 1997 *Stress Intensity Factors and Weight Functions* (*Advances in Fracture Series*) (Southampton: Computational Mechanics Publications) pp 275–7

Gall M and Thielicke B 2007 Life-span investigations of piezoceramic patch sensors and actuators *SPIE Conf. on Smart Structures and Materials & NDE 2007 (San Diego, CA), Behavior and Mechanics of Multifunctional and Composite Materials*; *Proc. SPIE* **6526** 65260P

Mall S 2002 Integrity of graphite/epoxy laminate embedded with piezoelectric sensor/actuator under monotonic and fatigue loads *Smart Mater. Struct.* **11** 527–33

Mall S and Hsu T L 2000 Electromechanical fatigue behavior of graphite/epoxy laminate embedded with piezoelectric actuator *Smart Mater. Struct.* **9** 78–84

Nuffer J *et al* 2008 Reliability investigation of adaptive systems for noise reduction on system and material level *Proc. Adaptronic Congr. 2008 (Berlin)* pp 155–64

Poizat C, Sester M, Thielicke B, Schönecker A and Keitel U 1999 Verbundwerkstoffe mit eingebetteten piezoelektrischen Fasern: modellierung und experimenteller Nachweis der sensorischen Wirkung *Werkstoffwoche98, symp 12* vol 1, ed K Kempter and J Haußelt pp 229–34

Santos e Lucato S L, Lupascu D C and Rödel J 2000 Effect of poling direction on R-curve behavior in lead zirconate titanate *J. Am. Ceram. Soc.* **83** 424–6

Thielicke B, Gesang T and Wierach P 2003 Reliability of piezoceramic patch sensors under cyclic mechanical loading *Smart Mater. Struct.* **12** 993–6

Wierach P, Monner H P, Schönecker A and Dürr J K 2002 Application specific design of adaptive structures with piezoceramic patch actuators *Proc. SPIE* **4698** 333–41

Wierach P and Schönecker A 2005 Bauweisen und anwendungen von piezokompositen in der adaptronik *Proc. Adaptronic Congr. 2005 (Göttingen)* paper 14

Yocum M, Abramovich H, Grunwald A and Mall S 2003 Fully reversed electromechanical fatigue behavior of composite laminate with embedded piezoelectric actuator/sensor *Smart Mater. Struct.* **12** 556–64